Spatial Attention Weakly Modulates Visual Responses in the Lateral Geniculate Nucleus

Henry J. Alitto[1,2+] Jeffrey S. Johnson[1,2], and W. Martin Usrey[1,2]

[1] Center for Neuroscience, University of California, Davis, Davis, CA, 95618, USA
[2] Neurobiology, Physiology, and Behavior University of California, Davis, Davis, CA, 95618, USA
[+] hjalitto@ucdavis.edu

Running title: Spatial attention in the LGN

Author Contributions: HJA and WMU designed the research, HJA performed the research, HJA and JSJ analyzed data, HJA and WMU wrote the paper

Number of Figures: 8
Number of Tables: 0
Number of Mulitmedia: 0
Number of words for Abstract: 247
Number of words for Significance Statement: 92
Number of words for Introduction: 597
Number of words for Discussion: 614

Acknowledgements: We thank K.E. Neverkovec, D.J. Sperka and R. Oates for expert technical assistance.

Conflict of Interest: Authors report no conflict of interest

Funding sources: This work was supported by NIH grants EY012576, EY036242, and P50MH132642

ABSTRACT

Visual responses in the cerebral cortex are strongly influenced by shifts in spatial attention. This modulation of visual processing includes changes in firing rate, decreased response variability, and decreased interneuronal correlations; all of which are thought to underlie enhanced visual perception near the center of attention at the cost of visual perception at other locations. Visual information from the retina is relayed to primary visual cortex via neurons in the lateral geniculate nucleus (LGN) of the dorsal thalamus. Although early studies describe an enhancement of LGN activity with spatial attention, more recent work has cast doubt on this view. Given its strategic position as the gateway to the cortex, an understanding of the effects of attention on visual processing in the LGN is important. We therefore performed experiments to reexamine the influence of covert spatial attention on the spiking activity of single units in the macaque LGN and applied a broad set of analyses and functional metrics to assess possible effects. Our results reveal a statistically significant effect of spatial attention in the LGN: firing rates were slightly higher and more reliable when monkeys directed attention towards the receptive fields of recorded neurons compared to when attention was directed to different retinotopic locations. However, effects were much smaller than previously reported (~1% vs ~4%) and further analyses suggest that effects are weak and inconsistent. Thus, while spatial attention does exert an influence in the LGN, its effects are weak and may have limited impact on downstream processing.

Significance Statement

The lateral geniculate nucleus (LGN) is a critical relay in the visual system, shaping the flow of sensory information from the eye to the brain. Although higher-order brain regions show strong modulation by attention, it remains unclear whether the LGN is similarly affected. By directly

recording LGN activity in monkeys performing a covert attention task, we found that spatial attention produces only weak and inconsistent modulation of visual responses. These findings suggest that the LGN largely operates independently of spatial attention, highlighting a potential boundary between early sensory processing and cognitive control.

Introduction

Spatial attention refers to the allocation of perceptual resources to enhance the processing of visual information at a specific spatial location, improving stimulus detectability and behavioral responsivity (Posner, 1980). While a full understanding of spatial attention is still emerging, the neural correlates of volitional spatial attention are generally believed to involve top-down processes (Maunsell, 2015; Boshra and Kastner, 2022; Martinez-Trujillo, 2022). These processes modulate fundamental aspects of visual responses in the cerebral cortex, including changes in firing rate, decreased response variability, and decreased neuronal correlations (Luck et al., 1997; McAdams and Reid, 2005; Cohen and Maunsell, 2009; Mitchell et al., 2009). Consistent with a top-down framework, the influence of spatial attention on visual response properties is greatest towards the top of the visual hierarchy (e.g., IT cortex) and weakest in primary visual cortex (V1), the initial stage of visual processing in the cortex (Luck et al., 1997; Kastner and Ungerleider, 2000; McAdams and Reid, 2005; Lauritzen et al., 2010; Ni and Maunsell, 2019; Meyyappan et al., 2025).

Along with the cortex, subcortical areas also play a role in spatial attention (Saalmann and Kastner, 2011; Zénon and Krauzlis, 2012; Zhou et al., 2016; Sherman and Usrey, 2021). Two of these areas, the superior colliculus in the midbrain and the pulvinar in the thalamus, receive strong, driving input from the cortex (Lynch et al., 1985; Sherman and Guillery, 2002; Cerkevich et al., 2014; Baldwin et al., 2017) and, thus, a route exists for cortical mechanisms to influence their response properties and communication with target structures. In contrast, neurons in the lateral geniculate nucleus (LGN) lack driving cortical input, instead receiving their driving input exclusively from the retina which is then relayed to cortex (reviewed in Usrey & Alitto, 2015) . Despite this, LGN activity has been reported to be influenced by spatial attention (O'Connor et al., 2002; McAlonan et al., 2008), potentially mediated by modulatory feedback pathways from the cortex and/or inhibitory circuits involving the thalamic reticular nucleus (TRN) (McAlonan et

al., 2008). The impact of attention on LGN activity remains unclear, though, as more recent work has not found effects of attention on visual processing in the LGN (Jiang et al., 2015; Shah et al., 2022).

Given the differences in past results and the importance of understanding the dynamics of visual signals delivered to cortex, we reexamined the influence of spatial attention on the spiking activity of LGN neurons in the macaque monkey and applied a broad set of analyses and functional metrics to assess possible effects. Moreover, recognizing that effects may be small, we collected data from a large sample of LGN neurons to strengthen the statistical analyses. Our results reveal small but significant effects of attention on the firing rate and reliability of LGN responses to visual stimuli. However, a deeper analysis of the data reveals that these effects are weak and inconsistent. Specifically, we found that shifting spatial attention towards LGN receptive fields was the equivalent of increasing the stimulus contrast by 1.25% or 1.0% for parvocellular and magnocellular neurons, respectively. Likewise, an ROC analysis indicates that an ideal observer would only be able to distinguish attend-toward trials from attend-away trials with 52% accuracy. Additionally, we did not observe a change in burst activity with shifts in spatial attention. Given that changes in burst firing are considered a reliable indicator of changes in thalamic network state (Sherman, 2001; McCormick et al., 2015), this is further evidence of the weak influence of spatial attention on LGN responses. Collectively, these results indicate that the modulation of LGN responses by spatial attention is statistically significant but functionally ineffectual.

MATERIALS AND METHODS

Two adult rhesus monkeys (Macaca mulatta; one male and one female) were used for electrophysiological recordings in this study. All experimental procedures conformed to the National Institutes of Health and the United States Department of Agriculture guidelines and were approved by the Institutional Animal Care and Use Committee at [**redacted for blind review**]. Under full surgical anesthesia, the animals received a cranial implant consisting of a head post for head stabilization and a recording cylinder that allowed access to the LGN.

Electrophysiological recordings. Extracellular recordings from the LGN were made with platinum-glass electrodes (1–2 MΩ; Alpha Omega) using a microdrive (40 mm electrode travel; Thomas Motorized Electrode Manipulator, Thomas Recording) mounted on the recording chamber. Online continuous voltage signals were amplified (A-M Systems), filtered (0.1–5 kHz), and recorded using a Micro1401 data acquisition system (28 kHz) and Spike2 software (Cambridge Electronic Design, CED). To extract action potentials, extracellular signals were high-pass filtered (stopband edge frequency = 500 Hz), thresholded, and clustered within the Spike2 software.

Visual Stimulation and Receptive Field Mapping. Visual stimuli were generated with a ViSaGe (Cambridge Research Systems) and presented on a gamma-corrected CRT monitor (Sony or Mitsubishi) positioned ~80 cm in front of the animal. The display had a resolution of 1024x768, a refresh rate of 100-140Hz, and a mean luminance of ~38 cd/m2. LGN receptive fields were manually mapped using small (<0.5°) user-controlled, computer-generated visual stimuli (custom software with Spike2 interface). The visual stimuli used for assessing spatial attention are described below.

Behavioral training and performance. Data was collected while the animals performed a spatial attention task (Figure 1A-B) while eye position and pupil size were monitored using an

Eye-Trac6 infrared eye tracker (Applied Science Laboratories) with a custom Spike2 interface. For this task, the animals initiated a trial by fixating a central fixation dot similar to the fixation dot used for passive fixation (hand mapping trials). The fixation dot was ~0.2° diameter, and the fixation window was 0.8°-1.2° diameter. After a short delay (0.5-1.0s), two sine wave gratings (temporal frequency = 5 Hz, spatial frequency = 1.0 cycles/°) appeared at equidistant locations from the fovea, typically at an eccentricity of 4-8°. Each sine wave grating was surrounded by a colored circle (one green, one red), and the color of the circles at each location was constant throughout the task. The color of the fixation dot (either red or green) indicated to the animal which grating was 90% likely to change contrast (valid trials) after a delay with an exponential hazard function of 0.6 – 1.8s. On 10% of the trials (invalid trials), the uncued grating increased in contrast (same hazard function). The base contrast of the grating was set to be near the C50 (contrast to evoke a half-maximum response) of the recorded LGN neuron, as estimated through hand mapping. After the contrast change, the animal was given 1s to respond by making a saccade to the location of the change, and the animal was rewarded with a small juice reward. Psychophysical performance (accuracy and reaction time) for valid and invalid trials were compared to ensure that the animals were applying spatial attention as anticipated. Based on these comparisons, the contrast change was titrated so that the animal performed 20-30% better on cued trials relative to uncued trials.

Analysis

Classification of neurons: Based on the hand-mapping procedures described above, we classified LGN neurons on two axes: cell-type and response polarity. Cell types were defined as magnocellular or parvocellular based on the C50 (C50 greater than 35% were classified as parvocellular, C50 less than 35% were classified as magnocellular). Response polarity (on-center cells vs off-center cells) was based on responses to increases and decreases in luminance.

Firing rate and spatial attention: LGN neurons have linear responses to the presentation of drifting sine wave gratings that are modulated by the phase of visual stimulus. To extract this linear response, we calculated the average cycle histogram (cycle duration = 200 ms, bin size = 7.7 ms) for each trial and extracted the linear response as the F_1 from a Fourier transform with a Hanning window (custom Matlab script). Based on the F_1 and F_0 (mean firing rate), the attention index was defined as:

$$attention\ index = (FR_{toward} - FR_{away})/(FR_{toward} + FR_{away})$$

Here, the FR is the firing rate (either the F_0 or F_1) during attend toward and attend away trials.

Equivalent Contrast Change: Shifts in spatial attention are often analogized as being similar to changes in stimulus contrast (Carrasco et al., 2004; Reynolds and Chelazzi, 2004). Given that shifts in spatial attention cause changes in the firing rates of visual neurons, we wanted to determine the changes in contrast that would have produced equivalent changes in firing rate. In the current study, the baseline stimulus contrast was individually specified for each LGN neuron, based on computer-aided hand mapping of the receptive field, to evoke 50% of the cell's maximum response (C50). Since complete contrast response functions were not available for the current data set, we created standardized parvocellular and magnocellular contrast response functions from a separate sample of LGN neurons (Figure 3a; magnocellular: n = 33, parvocellular: n = 87; 5-8 stimulus repeats per contrast) and applied the attentional changes in firing onto this value to determine an effective/equivalent contrast change. For each recorded neuron, we estimated the attention-driven change in firing rate as:

$$\Delta FR = \frac{FR_{toward} - FR_{away}}{FR_{toward}}$$

Using the standardized magnocellular and parvocellular contrast response functions, we then estimated the contrast that would have evoked an equivalent response difference relative to the

C50. For example, if the attend-toward firing rate was 1.2x greater than the attend-away firing rate, we would identify the contrast that would have evoked a response that was 1.2x the firing rate evoked at C50. Based on this calculation we then defined attention equivalent contrast change as:

$$\text{attention equivalent contrast change} = \frac{equivalent\ contrast - baseline\ contrast}{\text{baseline contrast}}$$

ROC analysis of attentional modulation: To further quantify the influence of spatial attention on visual responses in the LGN, we performed an ROC analysis to determine how well an ideal observer would be able to determine the focus of the animal's attention based solely on the trial-by-trial distribution of F_1s across attend-toward and attend-away trials. Using the matlab function perfcurve (bootstrap n = 1000), we determined if (a) attend toward trials were distinguishable from spontaneous activity, (b) attend away trials were toward trials were distinguishable from spontaneous activity, and (c) attend toward trials were distinguishable from attend away trials. For this analysis, spontaneous activity was based on the intertrial interval (ITI).

Influence of attention on thalamic Bursts: Spiking activity in the thalamus is often segregated into tonic and burst firing (Sherman, 2001). In tonic firing, thalamic neurons respond to excitatory stimuli in a linear, constant fashion where the mean firing rate is proportional to the strength of the stimulus. When thalamic neurons are sufficiently hyperpolarized to deinactivate T-type Ca^{++} channels, they begin to exhibit bursting activity (McCormick and Huguenard, 1992). As has been done previously (Reinagel et al., 1999; Alitto et al., 2019; Sanchez et al., 2023), we tracked burst and tonic firing based on the following criteria: (1) an ISI of >100 ms that preceded the first spike in a sequence, and (2) one or more subsequent spikes that followed with ISIs of <4 ms. Past studies applying these criteria to intracellular recordings show that events defined as bursts co-occur with T-channel plateau potentials (Lu et al., 1992). Based on these criteria, we estimated the modulation of thalamic burst firing in the LGN by spatial attention.

Modulation of response reliability by spatial attention: To quantify the influence of spatial attention on response reliability in the LGN, we calculated the Fano factor for both attend-toward and attend-away trials (custom Matlab function). Fano factor is a common measure of response reliability and is defined as:

$$Fano\ factor = \frac{spike\ count\ variance}{spike\ count\ mean}$$

Statistical tests: When testing for statistical differences between two populations, we performed bootstrap analyses to estimate median values, median difference values, 95% confidence intervals, and statistical significance. For this process, data were resampled with replacement 10,000 times while maintaining the original sample size in each resampling iteration. Within the text, statistics will be presented as:

median [95% confidence intervals]

for example:

toward trial F_1: 23.45 [19.23 - 29.85]

Where applicable, a bootstrap median difference estimation (BDE) is also provided. Throughout the Results, the distributions from bootstrap analyses are illustrated within the figures (e.g., Figure 1D-F). These histograms show the distribution of median values (or median difference values) generated from the 10,000 resamples with replacement. These distributions provide graphical estimates of effect size, variability, and statistical confidence. For within-neuron statistical tests, trials were shuffled across attention conditions (e.g., attend toward vs. attend away) and resampled with replacement 10,000 times per neuron. Statistical significance for each neuron was determined as the proportion of resampled values exceeding the observed effect size:

$$p = \frac{\sum_{i=1}^{10000} abs(median(resample_i)) \geq abs(observed)}{10000}$$

For sample-level statistical tests involving index values (e.g., attention index, burst index), significance was defined as the proportion of resampled values having the different sign as the observed value. Specifically, for an observed attention index >0, significance was calculated as:

$$p = \frac{\sum_{i=1}^{10000} median(resample_i) < 0}{10000}$$

For an observed attention index <0, significance was calculated as:

$$p = \frac{\sum_{i=1}^{10000} median(resample_i) > 0}{10000}$$

Results

To study the influence of attention on visual processing in the lateral geniculate nucleus (LGN), we trained two macaque monkeys (M1 and M2) to perform a spatial attention task (Figure 1A-B, see Materials and Methods). Briefly, the animals were trained to fixate on a colored dot while two drifting sinusoidal gratings, each surrounded by a thin colored circle, were shown in the periphery (mean eccentricity = 7.7°±3.3°, std). The contrast of the drifting gratings was held constant for a randomized interval (0.6s – 2.0s), at which point one of the gratings increased in contrast and the animal was rewarded for making a saccade to that location. The probability of each grating changing contrast was linked to the color of the fixation point. If the color of the fixation point matched the color of the surrounding circle, then that grating changed contrast on 90% of the trials (valid trials). On the remaining 10% of trials, the nonmatching grating changed contrast (invalid trials). Importantly, the color of the circles did not change from trial to trial; instead, the color of the fixation point changed. As expected, both monkeys were faster and more accurate on valid trials relative to invalid trials, indicating the animals were using covert spatial attention to perform the task (Figure 1 C-F; response latency: $valid_{M1}$ = 354ms [347 - 365], $invalid_{M1}$ = 390ms [361 - 405], BDE_{M1} = -34ms [-54 - -5], p_{M1} = 0.0094; $valid_{M2}$ = 301ms [298 - 303], $invalid_{M2}$ = 396ms [378 - 417], BDE_{M2} = -96ms [-117 - -77], $p_{M2} < 10^{-5}$); hit rate: $valid_{M1}$ = 0.949 [0.932 - 0.964], $invalid_{M1}$ = 0.749 [0.701 - 0.796], BDE_{M1} = 0.20 [0.152 - 0.249], $p_{M1} < 10^{-5}$; $valid_{M2}$ = 0.982 [0.979 - 0.985], $invalid_{M2}$ = 0.719 [0.672 - 0.767], BDE_{M2} = 0.263 [0.217 - 0.311], $p < 10^{-5}$).

To quantify the influence of spatial attention on the spiking activity of LGN neurons, we recorded the responses of 283 isolated single units (Figure 2, 103 magnocellular neurons, 180 parvocellular neurons; 151 off-cells, 132 on-cells) across both monkeys while they performed the spatial attention task. For each neuron, one of the drifting gratings was centered over the neuron's receptive field and the other grating was shown at an equidistant location from the

fixation point. Gratings were approximately 2-3 times the estimated size of the recorded neuron's classical receptive field (typically 2° in diameter). Across cells and illustrated with the examples shown in Figure 2, LGN responses to the drifting sine wave grating largely matched the drift frequency of the grating (5 Hz). Thus, as is standard, we primarily focused on this component (first harmonic, F_1) of the firing rate as quantified through Fourier analysis (see Materials and Methods).

Influence of spatial attention on neuronal firing rate

Across our sample of LGN neurons, there was a small, but significant, increase in the F_1 of the firing rate when the monkey directed attention toward the LGN cell's receptive field (toward trials) relative to when it directed attention away from the receptive field (away trials) (Figure 3). This effect was seen in M1 (Figure 3A-B (red data), toward = 26.1 [23.9 - 28.4] spikes/s, away = 25.2 [22.9 - 27.5] spikes/s, n = 161, BDE = 0.93 [0.56 - 1.32] spike/s, $p < 10^{-5}$) and M2 (Figure 3A-B (blue data), toward = 25.8 [23.1 - 28.4] spikes/s, away = 24.9 [22.255 - 27.476], n = 122, BDE = 0.48 [0.10 - 0.92] spikes/s, p = 0.0059). This effect was also seen when data were divided based on cell type (Figure 3C,D (parvocellular, red data), toward = 24.5 [22.8 – 26.2] spikes/s, away = 23.9 [22.2 – 25.7] spikes/s, BDE = 0.54 [0.24 – 0.84] spike/s, p = 0.0001; (magnocellular, blue data), toward = 29.1 [26.1 – 32.1] spikes/s, away = 28.0 [25.0 – 31.0], BDE = 1.1 [0.57 – 1.67] spikes/s, $p < 10^{-5}$) and luminance polarity (Figure E-F, (off-center, black data) toward = 26.9 [24.7 – 29.2] spikes/s, away = 26.2 [24.0 – 28.5], BDE = 0.72 [0.31 – 1.17] spikes/s, $p < 10^{-5}$; (on-center, red data), toward = 25.2 [23.0 – 27.4] spikes/s, away = 24.5 [22.4 – 26.7] spikes/s, BDE = 0.76 [0.43 - 1.1] spikes/s, $p < 10^{-5}$). The differences between parvocellular vs magnocellular (BDE = -0.16 [-0.73 – 0.33] spike/s, p = 0.31) and on-center vs off-center (BDE = 0.12 [-0.36 – 0.60] spikes/s, p = 0.65) were not statistically significant. Similar differences were seen for the mean response (F_0; data not shown), for M1 (toward = 27.4 [24.9 - 30.0] spikes/sec, away = 26.5 [24.0 - 29.0] spikes/sec, BDE = 0.92 [0.54 - 1.32] spikes/s, $p < 10^{-}$

^{5}) and M2 (toward = 30.6 [27.7 - 33.4] spikes/s, away = 30.0 [27.2 - 32.9] spikes/s, BDE = 0.54 [0.06 - 1.08] spikes/s, $p < 0.0114$). Across monkeys and cell types, the influence of attention on firing rate was significant, but small, increasing firing rate by ~ 1 spike/s.

Given that the firing rate varies from cell to cell, a bounded index is often useful for making comparisons between conditions across a sample of cells. We therefore used an attention index based on each cell's F_1 response, where

$$attention\ index = \frac{FR_{toward} - FR_{away}}{FR_{toward} + FR_{away}}$$

With the attention index, positive values indicate the firing rate increased with attention directed towards the neuron's receptive field and negative values indicate the firing rate decreased with attention. For both monkeys, median attention index values were significantly greater than zero (Figure 4A, D-E; M1: 0.014 [0.011 - 0.022], $p < 10^{-5}$; M2: 0.01 [0.001 - 0.012], $p = 0.0009$). When data was combined across monkeys an increased attention index was evident for parvocellular neurons (Figure 4F-G, 0.011 [0.003 - 0.015], $p = 0.0004$, $n = 180$), magnocellular neurons (Figure 4F-G, 0.012 [0.009 - 0.020], $p < 10^{-5}$, $n = 103$), on-cells (Figure 4H-I, 0.012 [0.007 - 0.018], $p < 10^{-5}$, $n = 131$), and off-cells (Figure 4H-I, 0.012 [0.004 - 0.015], $p < 10^{-5}$, $n = 152$). The differences between parvocellular and magnocellular neurons (parvocellular – magnocellular: -0.002 [-0.012 - 0.004], $p = 0.22$) as well as between on-center and off-center neurons (on-center – off-center: 0.001 [-0.006 - 0.009], $p = 0.41$) were not statistically significant. On a cell-by-cell basis, 16.6% of cells (47/283) had a statistically significant attention index at a significance level of 0.05 (Figure 4B). This distribution of statistically significant cells was marginally biased (Figure 4C, $p = 0.0479$) toward significantly positive attention index values (11.1% of cells) compared to significantly negative attention values (5.3% of cells). For the remainder of the paper, no statistically significant differences were seen between on-center and off-center data. Thus, on-center vs off-center differences will not be discussed.

Given that the influence of attention on firing rates appeared to be relatively small, we wished to put this change into perspective and estimate its functional relevance. Since spatial attention is often viewed as effectively increasing the contrast of the visual stimuli at that attended location, we wanted to determine the change in stimulus contrast that would evoke the same change in firing rate as shifting spatial attention toward the LGN receptive field (Figure 5). We therefore calculated the attention equivalent contrast change (AECC, see Materials and Methods). In the current study, the baseline contrast was set to be at the neuron's C50 (the contrast that evoked a half-maximum response), but since each neuron's C50 was estimated online with hand-mapping procedures, we used data from a separate population of neurons to generate standardized contrast response functions for magnocellular (n = 33) and parvocellular (n = 87) neurons (Figure 5A). Using these standardized functions, we calculated the contrast, relative to the C50, that evoked the same change in firing rate as shifting spatial attention. For example, if the change in firing rate caused by shifting attention was equivalent to the change in firing rate caused by increasing the contrast from 30% to 40%, then the AECC would be 0.33. For the parvocellular neurons in this study (Figure 5B-D), the 0.52 [0.097 - 0.785] spikes/s increase in firing when spatial attention was shifted toward the cell's receptive field is equivalent to a relative increase in contrast of only 0.025 [0.017 - 0.032] that is a change equal to 2.5% of the C50. For a typical parvocellular neuron, this would be the equivalent of changing the contrast from 50.0% to 51.25%. For magnocellular neurons (Figure 5B-D), the 0.681 [0.294 - 1.112] spikes/s increase in firing rate with attention is equivalent to a relative increase in contrast of 0.058 [0.041 - 0.076]. For a typical C50 seen in magnocellular neurons, this would be the equivalent of changing the contrast from 18.0 to 19.0. Across cells, equivalent contrast change values were significantly greater for magnocellular neurons than for parvocellular neurons (magno - parvo: 0.033 [0.014 - 0.052] p = 0.0002); however, for both cell types the equivalent contrast change values were very small and likely would be below threshold for change detection.

A separate metric that can be applied to assess the influence of spatial attention on visual responses utilizes receiver operating characteristic (ROC) analysis (Figure 6). With ROC analysis, one can ask how well an ideal observer would be able to determine, on a cell-by-cell basis, where the monkey was focusing its attention based solely on the response distributions (see Materials and Methods). A small difference in mean response would be discernable if there was also little variability (e.g., all trials with attention towards the cell's RF had the same small difference in firing rate compared to all away trials). At the opposite extreme, the same small difference in mean response would not be discernable if associated with much greater variability. In the first case with low variance, the ideal observer would successfully distinguish attend-towards and attend-away trials a high percent of the time. In the second case, the ideal observer would do much worse. Applying this approach, results indicate an ideal observer would have no difficulty discriminating either toward or away trial contrast changes from the baseline contrast (Figure 6A-B, D-I, toward = 0.912 [0.898 - 0.925], $p < 10^{-5}$; away = 0.902 [0.888 - 0.916], $p < 10^{-5}$). On a cell-by-cell basis, 97.2% of cells had a statistically significant toward trial vs baseline AUC and 96.5% of cells had a statistically significant away trial vs baseline AUC ($p<0.05$). However, and more importantly, the same methodology revealed that toward and away trials could only be discriminated with an accuracy of 0.522 (Figure 6C, 0.522 [0.513 - 0.532]). On a cell-by-cell basis, only 13.8% of cells had statistically significant toward vs away AUC ($p<0.05$). However, it is worth nothing that significant AUCs were more common ($p = 0.01$) for cells with greater activity while attending toward the LGN RF (n = 28, 9.9% of cells) compared to cells with greater activity while attending away from the LGN RF (n = 11, 3.9% of cells). Overall, these results indicate the influence of spatial attention in the LGN is weak and not a reliable indicator of where the animal was attending on a trial-to-trial basis.

Spatial attention and thalamic bursts

Across thalamic nuclei, relay cells produce spikes that can be categorized as burst spikes or tonic spikes (Sherman, 2001). Although burst spikes are less common in alert animals compared to anesthetized animals (Glenn and Steriade, 1982; Ramcharan et al., 2000; Alitto et al., 2011), spatial attention could serve to modulate the relative occurrence of burst and tonic spikes. Consistent with previous studies, results from this study show that burst spikes were infrequent in the alert animal (Figure 7A). This was the case for trials when animals were directed to attend towards the recorded cells' receptive fields (proportion burst spikes: all cells = 0.017 [0.015 - 0.018], M1 = 0.018 [0.016 - 0.021]; M2 = 0.014 [0.011 - 0.017], parvocellular cells = 0.018 [0.015 - 0.020], magnocellular cells = 0.016 [0.013 - 0.019]) and away from the recorded cells' receptive fields (proportion burst spikes: all cells = 0.016 [0.015 - 0.018]; M1 = 0.018 [0.016 - 0.021]; M2 = 0.015 [0.012 - 0.017], parvocellular cells = 0.017 [0.015 - 0.020]; magnocellular cells = 0.016 [0.013 - 0.019]). Further, shifts in spatial attention did not significantly modulate the probability of an LGN neuron firing in burst mode as assessed using a burst index:

$$burst\ index = \frac{(BP_{toward} - BP_{away}}{(BP_{toward} + BP_{away})}$$

(Figure 7B-D; burst index: M1 = 0.027 [-0.034 - 0.0088], p = 0.27; M2 = -0.004 [-0.074 - 0.061], p = 0.44; parvocellular cells = -0.017 [-0.072 - 0.029], p = 0.35; magnocellular cells = -0.009 [-0.088 - 0.009], p = 0.32). On a cell-by-cell basis, 11.7% of cells (33/283) had significant burst index values, evenly split between more bursts during attend-toward trials (5.6%) and more bursts during attend-away trials (6.0%) at a significance level of 0.05. There was, however, a significant negative correlation between the firing rate of recorded cells and burst percent for both toward trials (Figure 7E,F; r = -0.15 [-0.247 - -0.055], p = 0.001) and away trials (r = -0.17 [-0.259 - -0.070], p = 0.0005). This inverse relationship might be explained by the time-voltage relationship that governs the production of bursts which, in turn, may reflect variable levels of

alertness across/within recording sessions. Importantly, there was no correlation between burst rate and the magnitude of spatial attention effects on the firing rate of LGN cells (r = 0.03 [-0.150 - 0.091], p = 0.31).

Influence of spatial attention on response reliability

Past studies have shown that spatial attention increases response reliability in visual cortex (Mitchell et al., 2007); however, this effect has not been previously demonstrated in the LGN. To examine the influence of spatial attention on LGN response reliability, we calculated the Fano factor (Fano factor = spike count variance / spike count mean) when animals were directed to attend towards and away from the recorded neurons' receptive fields (Figure 8). Consistent with results from studies not examining attention (Kara et al., 2000; Alitto et al., 2011), Fano factors across our sample of LGN neurons were, on average, below 1.0, indicating the responses of LGN neurons are less variable than expected from a Poisson process. This was the case for trials when animals were cued to attend towards the recorded cells' receptive fields (Figure 8A, Fano factor: M1 = 0.928 [0.908 - 0.958]; M2 = 0.924 [0.897 - 0.951], parvocellular cells = 0.932 [0.900 - 0.955]; magnocellular cells = 0.922 [0.908 - 0.968]; and away from the recorded cells' receptive fields (Fano factor: M1 = 0.92 [0.91 - 0.94], M2 = 0.95 [0.90 - 0.98], parvocellular cells = 0.932 [0.900 - 0.955]; magnocellular cells = 0.922 [0.908 - 0.968]). Although Fano factors were extremely similar for attend towards and attend away trials, there was a significant decrease in the Fano factor (as assessed using a Fano factor index, see Materials and Methods) when attention was directed towards the receptive fields of recorded neurons (Figure 8B-D); FF Index: M1 = -0.005 [-0.010 - 0.000], p = 0.0306; M2 = -0.008 [-0.013 - -0.003], p = 0.0003; parvocellular cells = -0.004 [-0.008 - 0.000], p= 0.036; magnocellular cells = -0.010 [-0.016 - -0.004], p = 0.0005). On a cell-by-cell basis 21.9% of cells had statistically significant Fano factor index values (62/283), at a significant level of 0.05, with a significant bias (p = 0.0002) toward more cells with significantly negative FF index values (18%, more reliable during

attend-toward trials) compared cells with significantly positive FF index values (4.6%, more reliable during attend away trials). Thus, similar to the effects of attention on firing rate, there was a small, but significant, influence of attention on the response reliability of LGN neurons.

Discussion

It is generally agreed that the central nervous system lacks the resources to process all visual information that falls on the retina. Instead, the processing of behaviorally relevant information is prioritized at the expense of other, less or non-relevant visual information. Spatial attention, the preferential processing of visual stimuli at a specific spatial location, is one mechanism that has a profound influence on what sensory information enters conscious perception. While early studies reported moderate attentional modulation in the lateral geniculate nucleus (LGN)—including increased BOLD signal in humans and enhanced parvocellular/magnocellular firing rates in primates (O'Connor et al., 2002; McAlonan et al., 2008) —subsequent findings have indicated otherwise (Jiang et al., 2015; Shah et al., 2022). Notably, Shah et al. (2022) did not find effects of attention in the LGN, despite observing strong attentional modulation in V1.

While the results reported here confirm that spatial attention does influence LGN activity (Figures 2 and 6), a deeper analysis of the data indicates that these effects are weak and inconsistent (Figures 3-5). The observed firing rate increases (on average, ~1 spike/s) corresponded to only a 1–1.8% contrast change, and ROC analysis showed that an ideal observer could barely distinguish attend-toward from attend-away trials (*53% accuracy*). Furthermore, burst firing, a key indicator of thalamic network state, remained unchanged. Collectively, these findings suggest that spatial attention has a statistically significant but functionally negligible effect on LGN processing.

Given its position between the retina and cortex (Usrey and Alitto, 2015), the LGN might seem like an ideal site for attentional gating. Its small receptive fields could, in theory, support a highly retinotopically precise spotlight of attention, which becomes harder to achieve in higher-order cortex where receptive fields are larger. However, this is not how the visual system operates. Instead, attentional modulation is strongest in higher-order areas (e.g., IT, MT) (Connor et al., 1997; Seidemann and Newsome, 1999; Treue and Maunsell, 1999;

Ramezanpour and Fallah, 2022) and weakest at the early stages of processing (Luck et al., 1997; Shah et al., 2022).

One possible reason is that early visual areas serve as a preprocessing hub, establishing a basis set for the encoding of natural images that is robust against changes in basic stimulus properties such as luminance and contrast (Shapley and Victor, 1979; Heeger, 1992; Olshausen and Field, 1996; Alitto and Usrey, 2004; Bonin et al., 2005; Priebe and Ferster, 2012). When visual information reaches the cortex, V1 acts as a distribution hub sending visual information down a variety of parallel pathways, each of which builds upon the relatively simple, spatially compact receptive fields found in the early visual system, ultimately resulting in a unified perception of the visual world (Felleman and Van Essen, 1991). Strong attentional modulation at the LGN stage might introduce undesirable, nonspecific filtering, affecting all downstream visual pathways indiscriminately. A more efficient strategy is to reserve strong attentional modulation for higher-order areas where receptive fields are already task-tuned—for example, MT during motion discrimination or FFA during face recognition. Thus, in the context of spatial attention, the role of the LGN is to maintain a stable, unbiased flow of retinal input to V1, where visual information is distributed across parallel processing streams before attentional filtering occurs at later stages.

A parallel can be drawn to arousal-driven LGN modulation, which globally enhances or suppresses visual signals depending on behavioral state (Molnár et al., 2021; Crombie et al., 2024). Unlike spatial attention, arousal-based modulation affects all LGN neurons indiscriminately, ensuring coordinated gain control rather than interfering with specific spatial and/or feature-processing streams. Similarly, LGN activity is suppressed during modality-specific attention to non-visual tasks, a scenario where broad suppression is beneficial rather than disruptive (Wimmer et al., 2015).

Figure Legends

Figure 1. Spatial attention task and psychophysical measure of spatial attention. Two macaque monkeys (M1 and M2) were trained to perform a covert spatial attention task. ***A***. On each trial, animals maintained fixation on a central green dot while two peripheral sine wave gratings appeared, each surrounded by a colored circle. One grating was positioned over the receptive field of a recorded LGN neurons and the other at an equidistant location. The color of the fixation point, in conjunction with the colors of the peripheral circles, indicated the probability that each grating would undergo a contrast increase after a brief delay. ***B***. In 90% of trials (valid), the contrast change occurred at the location where the circle color matched the fixation cue. In 10% of trials (invalid, not shown), the contrast change occurred at the non-matching location. Animals were rewarded for making a saccade to the grating that increased in contrast. Both animals respond faster (***C, D***) and more accurately (***E, F***) on valid trials compared to invalid trials. Statistical significance was assessed using bootstrap difference estimation (BDE). Panels D and F show the distribution of median differences (valid – invalid) computed over 10,000 bootstrap resamples for M1 (red) and M2 (blue). These distributions provide graphical estimates of effect size, variability, and statistical confidence (see Methods and Materials for details).

Figure 2. Single-unit examples of lateral geniculate nucleus (LGN) responses recorded while the animal performed the spatial attention task. Each row (***A - F***) shows data from one neuron. ***Column 1***. Peri-stimulus time histograms (PSTHs) showing firing rates for valid *attend-toward* (red) and *attend-away* (blue) trials, aligned to the time of contrast change (0 s). ***Column 2***. Mean firing rate across all trials as a function of time relative to the start of recording. ***Column 3***. Distribution of firing rates (F_1) across all trials. ***Column 4***. Cumulative distribution of firing rates across all trials.

Figure 3. Firing rate during spatial attention. ***A***. Distribution of firing rates (f1) for attend toward vs attend away trials across all cells (M1 = red, M2 = blue; n = 283). ***B***. Significance of these effects was determined via a bootstrap difference estimation (See Materials and Methods). The red and blue data in panel ***B*** show the distribution of median difference values (toward – away) over 10,000 resamples with replacement for M1 and M2, respectively. These distributions provide a direct graphical illustration of statistical significance and confidence intervals (p values in text). ***C, D***. Same as ***A, B*** for parvocellular (red) and magnocellular (blue) data. ***E, F***. Same as ***A, B*** for on-center (red) and off-center (black).

Figure 4. Attention index. ***A***. Distribution of attention index values across cell types. ***B***. Overall distribution of attention index values. Significant values ($p < 0.05$) are indicated in black. ***C***. Significance of the distribution of attention index values (positive > negative) was determined by a bootstrap null distribution analysis (red dashed line = observed difference). ***D***. Distribution of attention index values for M1 (red) and M2 (blue) (0 = black dashed line). ***E***. Significance of these distributions was determined via a bootstrap mean estimation. ***F, G***. Same as ***D, E*** for parvocellular (red) and magnocellular (blue) data. ***H, I***. Same as ***A, B*** for on-center (red) and off-center (black) data.

Figure 5. Equivalent contrast change. ***A***. Population contrast response functions for parvocellular (red) and magnocellular (blue) data. ***B, C***. Distribution of equivalent contrast values across cell types. ***D***. Significance of these distributions was determined via a bootstrap mean estimation.

Figure 6. ROC analysis of spatial attention. ***A***. Area under the curve (AUC) for attend toward trials vs baseline, across cell types. ***B***. Area under the curve for attend away trials vs baseline, across cell types. ***C***. Area under the curve for attend toward trials vs attend away trials, across cell types. ***D***. Distribution of AUC values for M1 (red = toward vs baseline, blue = away vs

baseline, black = toward vs away). ***E***. Same as ***D*** for M2. F. Same as ***D*** for parvocellular data. ***G***. Same as ***D*** for magnocellular data.

Figure 7. Thalamic bursts during spatial attention. ***A***. Distribution of thalamic burst percentage for attend toward trials vs attend away trials. ***B***. Sample distributions for burst index values across cell types. ***C, D***. Significance of these effects illustrated via a bootstrap difference estimation. ***E***. Correlation between burst percentage and firing rate across all cell types (red = attend toward trials, blue = attend away trials, dashed line = linear fit). ***F.*** Significance of these correlations illustrated via a bootstrap mean estimation.

Figure 8. Response reliability during spatial attention. ***A***. Distribution of Fano factor values for attend toward trials vs attend away trials. ***B***. Sample distributions for Fano factor index values across cell types. ***C, D***. Significance of these effects as illustrated via a bootstrap difference estimation.

References

Alitto H, Rathbun DL, Vandeleest JJ, Alexander PC, Usrey WM (2019) The augmentation of retinogeniculate communication during thalamic burst mode. J Neurosci 39:5697–5710.

Alitto HJ, Moore BD, Rathbun DL, Usrey WM (2011) A comparison of visual responses in the lateral geniculate nucleus of alert and anaesthetized macaque monkeys. J Physiol 589:87–99.

Alitto HJ, Usrey WM (2004) Influence of contrast on orientation and temporal frequency tuning in ferret primary visual cortex. J Neurophysiol 91:2797–808.

Baldwin MKL, Balaram P, Kaas JH (2017) The evolution and functions of nuclei of the visual pulvinar in primates. J Comp Neurol 525:3207–3226.

Bonin V, Mante V, Carandini M (2005) The suppressive field of neurons in lateral geniculate nucleus. J Neurosci 25:10844–10856.

Boshra R, Kastner S (2022) Attention control in the primate brain. Curr Opin Neurobiol 76:102605.

Carrasco M, Ling S, Read S (2004) Attention alters appearance. Nat Neurosci 7:308–313.

Cerkevich CM, Lyon DC, Balaram P, Kaas JH (2014) Distribution of cortical neurons projecting to the superior colliculus in macaque monkeys. Eye Brain 6:121–137.

Cohen MR, Maunsell JHR (2009) Attention improves performance primarily by reducing interneuronal correlations. Nat Neurosci 12:1594–1600.

Connor CE, Preddie DC, Gallant JL, Van Essen DC (1997) Spatial Attention Effects in Macaque Area V4. J Neurosci 17:3201–3214.

Crombie D, Spacek MA, Leibold C, Busse L (2024) Spiking activity in the visual thalamus is

coupled to pupil dynamics across temporal scales. PLoS Biol 22:e3002614.

Felleman DJ, Van Essen DC (1991) Distributed hierarchical processing in the primate cerebral cortex. Cereb Cortex 1:1–47.

Glenn LL, Steriade M (1982) Discharge rate and excitability of cortically projecting intralaminar thalamic neurons during waking and sleep states. J Neurosci 2:1387–1404.

Heeger DJ (1992) Normalization of cell responses in cat striate cortex. Vis Neurosci 9:181–197.

Jiang Y, Yampolsky D, Purushothaman G, Casagrande VA (2015) Perceptual decision related activity in the lateral geniculate nucleus. J Neurophysiol 114:717–735.

Kara P, Reinagel P, Reid RC (2000) Low response variability in simultaneously recorded retinal, thalamic, and cortical neurons. Neuron 27:635–646.

Kastner S, Ungerleider LG (2000) Mechanisms of visual attention in the human cortex. Annu Rev Neurosci.

Lauritzen TZ, Ales JM, Wade AR (2010) The effects of visuospatial attention measured across visual cortex using source-imaged, steady-state EEG. J Vis 10.

Lu SM, Guido W, Sherman SM (1992) Effects of membrane voltage on receptive field properties of lateral geniculate neurons in the cat: Contributions of the low-threshold Ca2+ conductance. J Neurophysiol 68:2185–2198.

Luck SJ, Chelazzi L, Hillyard SA, Desimone R (1997) Neural mechanisms of spatial selective attention in areas V1, V2, and V4 of macaque visual cortex. J Neurophysiol 77:24–42.

Lynch JC, Graybiel AM, Lobeck LJ (1985) The differential projection of two cytoarchitectonic subregions of the inferior parietal lobule of macaque upon the deep layers of the superior colliculus. J Comp Neurol 235:241–254.

Martinez-Trujillo J (2022) Visual Attention in the Prefrontal Cortex. Annu Rev Vis Sci 8:407–425.

Maunsell JHR (2015) Neuronal Mechanisms of Visual Attention. Annu Rev Vis Sci 1:373–391.

McAdams CJ, Reid RC (2005) Attention modulates the responses of simple cells in monkey primary visual cortex. J Neurosci 25:11023–11033.

McAlonan K, Cavanaugh J, Wurtz RH (2008) Guarding the gateway to cortex with attention in visual thalamus. Nature 456:391–394.

McCormick DA, Huguenard JR (1992) A model of the electrophysiological properties of thalamocortical relay neurons. J Neurophysiol 68:1384–1400.

McCormick DA, McGinley MJ, Salkoff DB (2015) Brain state dependent activity in the cortex and thalamus. Curr Opin Neurobiol.

Meyyappan S, Rajan A, Yang Q, Mangun GR, Ding M (2025) Decoding Visual Spatial Attention Control. eNeuro 12.

Mitchell JF, Sundberg KA, Reynolds JH (2009) Spatial Attention Decorrelates Intrinsic Activity Fluctuations in Macaque Area V4. Neuron 63:879–888.

Mitchell JF, Sundberg KA, Reynolds JH (2007) Differential attention-dependent response modulation across cell classes in macaque visual area V4. Neuron 55:131–141.

Molnár B, Sere P, Bordé S, Koós K, Zsigri N, Horváth P, Lőrincz ML (2021) Cell Type-Specific Arousal-Dependent Modulation of Thalamic Activity in the Lateral Geniculate Nucleus. Cereb cortex Commun 2:tgab020.

Ni AM, Maunsell JHR (2019) Neuronal Effects of Spatial and Feature Attention Differ Due to Normalization. J Neurosci 39:5493–5505.

O'Connor DH, Fukui MM, Pinsk MA, Kastner S (2002) Attention modulates responses in the

human lateral geniculate nucleus. Nat Neurosci 5:1203–1209.

Olshausen BA, Field DJ (1996) Emergence of simple-cell receptive field properties by learning a sparse code for natural images. Nature 381:607–609.

Posner MI (1980) Orienting of attention. Q J Exp Psychol 32:3–25.

Priebe NJ, Ferster D (2012) Mechanisms of neuronal computation in mammalian visual cortex. Neuron 75:194–208.

Ramcharan EJ, Gnadt JW, Sherman SM (2000) Burst and tonic firing in thalamic cells of unanesthetized, behaving monkeys. Vis Neurosci 17:55–62.

Ramezanpour H, Fallah M (2022) The role of temporal cortex in the control of attention. Curr Res Neurobiol 3:100038.

Reinagel P, Godwin D, Sherman SM, Koch C (1999) Encoding of visual information by LGN bursts. J Neurophysiol 81:2558–2569.

Reynolds JH, Chelazzi L (2004) Attentional modulation of visual processing. Annu Rev Neurosci 27:611–647.

Saalmann YB, Kastner S (2011) Cognitive and perceptual functions of the visual thalamus. Neuron 71:209–223.

Sanchez AN, Alitto HJ, Rathbun DL, Fisher TG, Usrey WM (2023) Stimulus contrast modulates burst activity in the lateral geniculate nucleus. Curr Res Neurobiol 4:100096.

Seidemann E, Newsome WT (1999) Effect of spatial attention on the responses of area MT neurons. J Neurophysiol 81:1783–1794.

Shah S, Mancarella M, Hembrook-Short JR, Mock VL, Briggs F (2022) Attention differentially modulates multiunit activity in the lateral geniculate nucleus and V1 of macaque monkeys.

J Comp Neurol 530:1064–1080.

Shapley RM, Victor JD (1979) Nonlinear spatial summation and the contrast gain control of cat retinal ganglion cells. J Physiol 290:141–161.

Sherman SM (2001) Tonic and burst firing: dual modes of thalamocortical relay. Trends Neurosci 24:122–126.

Sherman SM, Guillery RW (2002) The role of the thalamus in the flow of information to the cortex. Philos Trans R Soc London Ser B, Biol Sci 357:1695–1708.

Sherman SM, Usrey WM (2021) Cortical control of behavior and attention from an evolutionary perspective. Neuron 109:3048–3054.

Treue S, Maunsell JH (1999) Effects of attention on the processing of motion in macaque middle temporal and medial superior temporal visual cortical areas. J Neurosci Off J Soc Neurosci 19:7591–7602.

Usrey WM, Alitto HJ (2015) Visual Functions of the Thalamus. Annu Rev Vis Sci 1:351–371.

Wimmer RD, Schmitt LI, Davidson TJ, Nakajima M, Deisseroth K, Halassa MM (2015) Thalamic control of sensory selection in divided attention. Nature 526:705–709.

Zénon A, Krauzlis RJ (2012) Attention deficits without cortical neuronal deficits. Nature 489:434–437.

Zhou H, Schafer RJ, Desimone R (2016) Pulvinar-Cortex Interactions in Vision and Attention. Neuron 89:209–220.

Figure 1

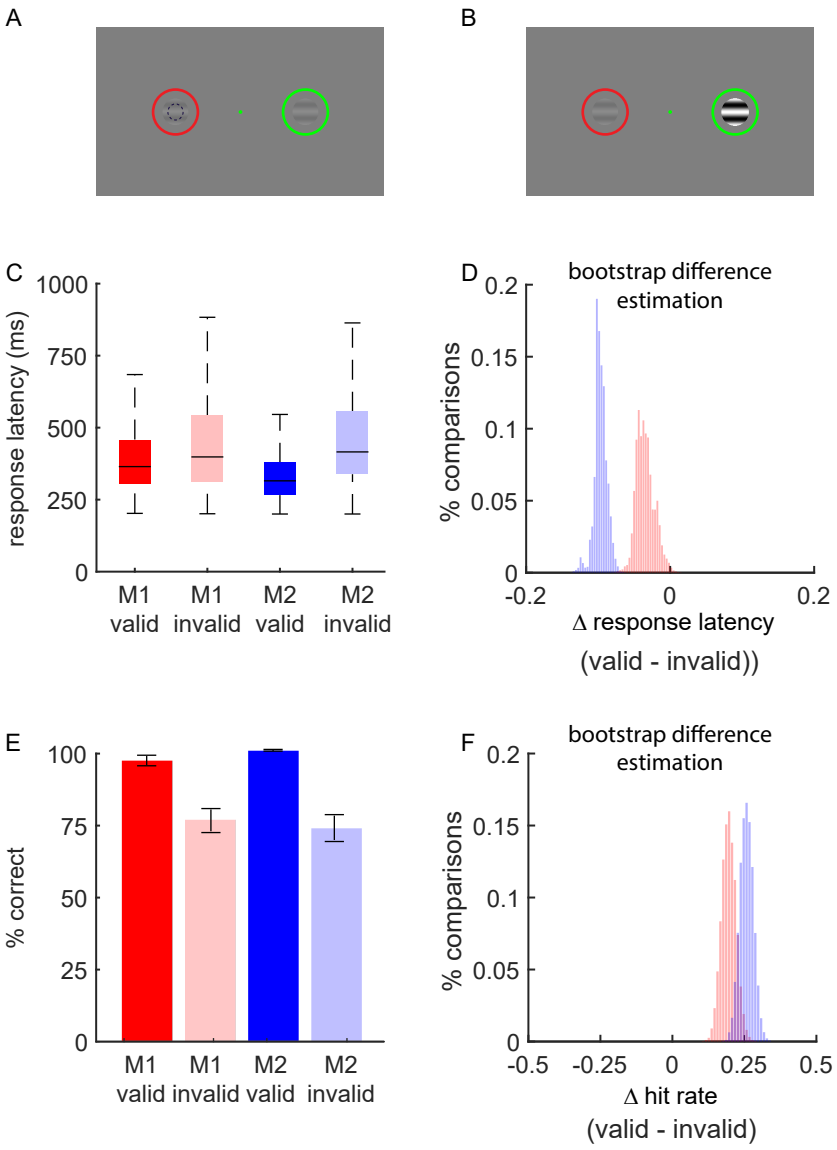
A
B
C
1000
750
500
250
0
response latency (ms)
M1 valid
M1 invalid
M2 valid
M2 invalid
D
bootstrap difference estimation
0.2
0.15
0.1
0.05
0
% comparisons
-0.2
0
0.2
Δ response latency
(valid - invalid))
E
100
75
50
25
0
% correct
M1 valid
M1 invalid
M2 valid
M2 invalid
F
bootstrap difference estimation
0.2
0.15
0.1
0.05
0
% comparisons
-0.5
-0.25
0
0.25
0.5
Δ hit rate
(valid - invalid)

Figure 2

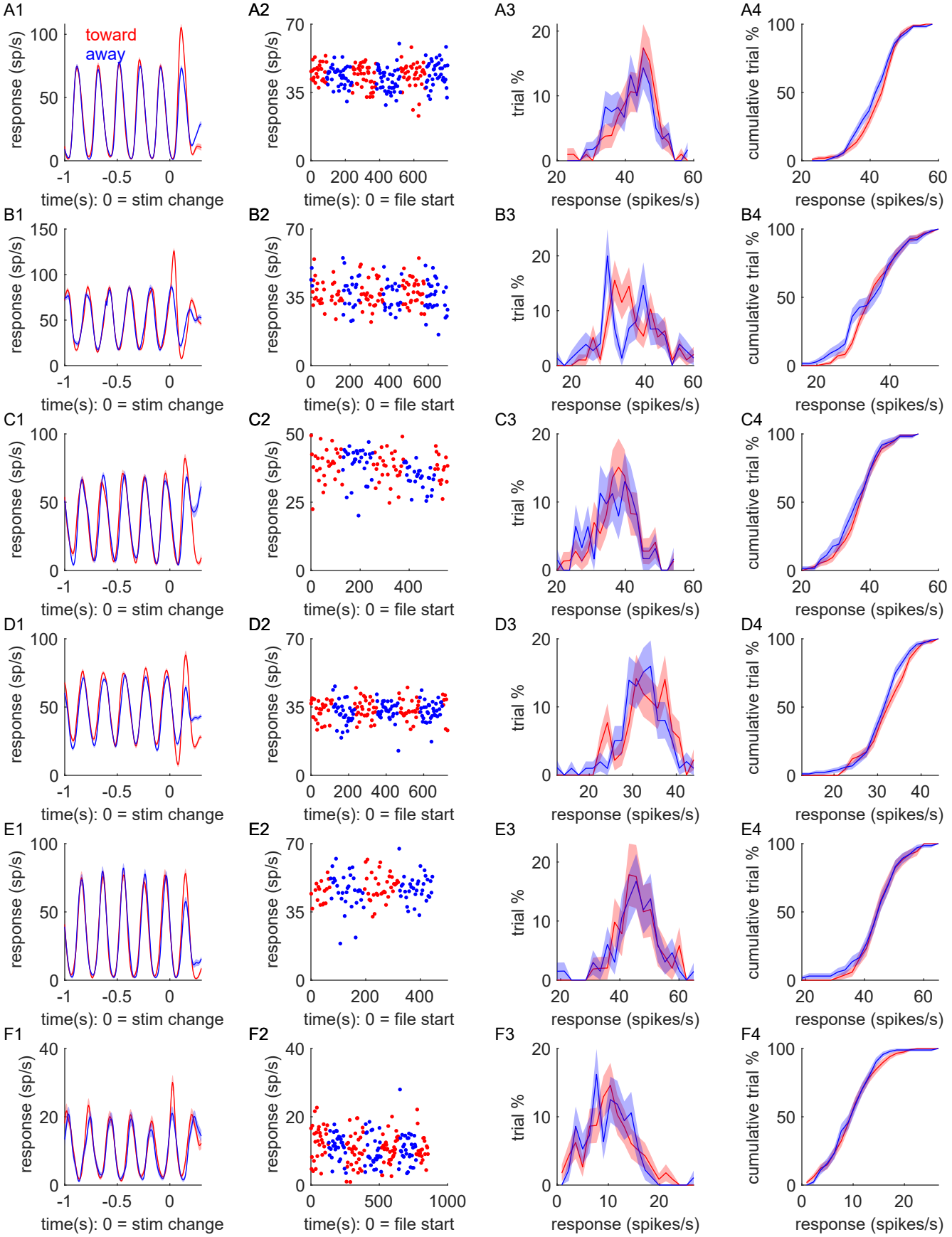
A1
toward
away
response (sp/s)
time(s): 0 = stim change
A2
response (sp/s)
time(s): 0 = file start
A3
trial %
response (spikes/s)
A4
cumulative trial %
response (spikes/s)
B1
B2
B3
B4
C1
C2
C3
C4
D1
D2
D3
D4
E1
E2
E3
E4
F1
F2
F3
F4

Figure 3

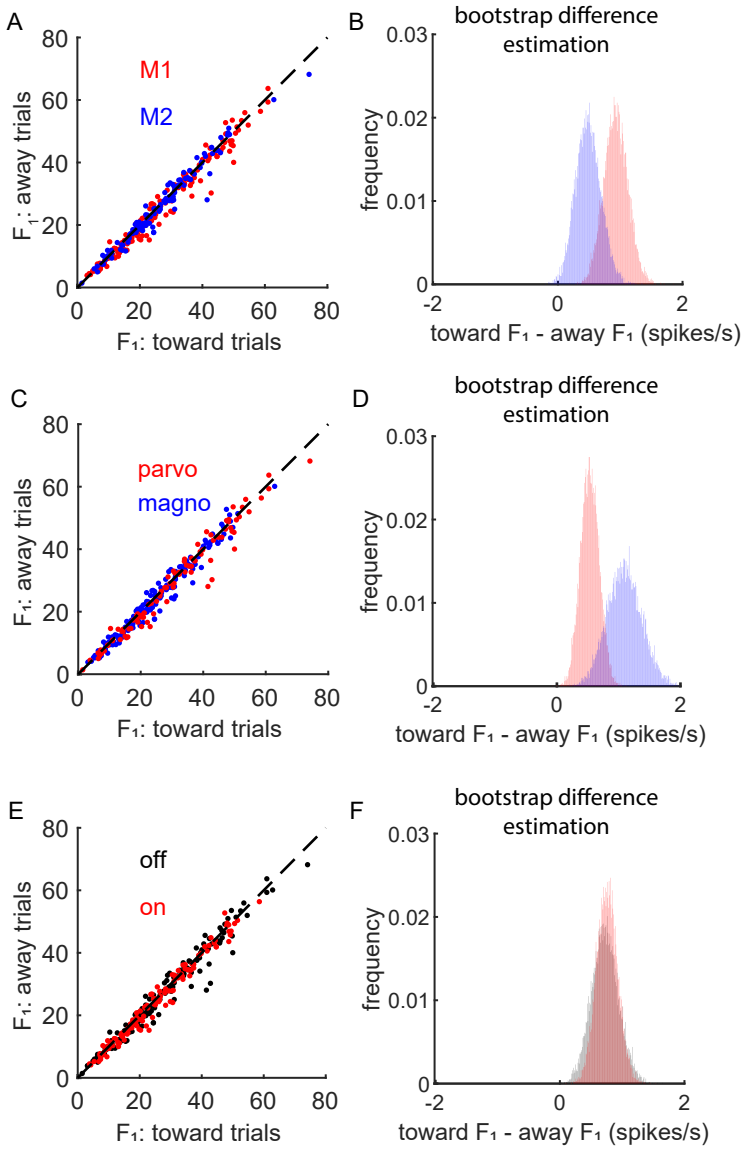
A
M1
M2
F1: away trials
F1: toward trials
B
bootstrap difference estimation
frequency
toward F1 - away F1 (spikes/s)
C
parvo
magno
D
E
off
on
F

Figure 4

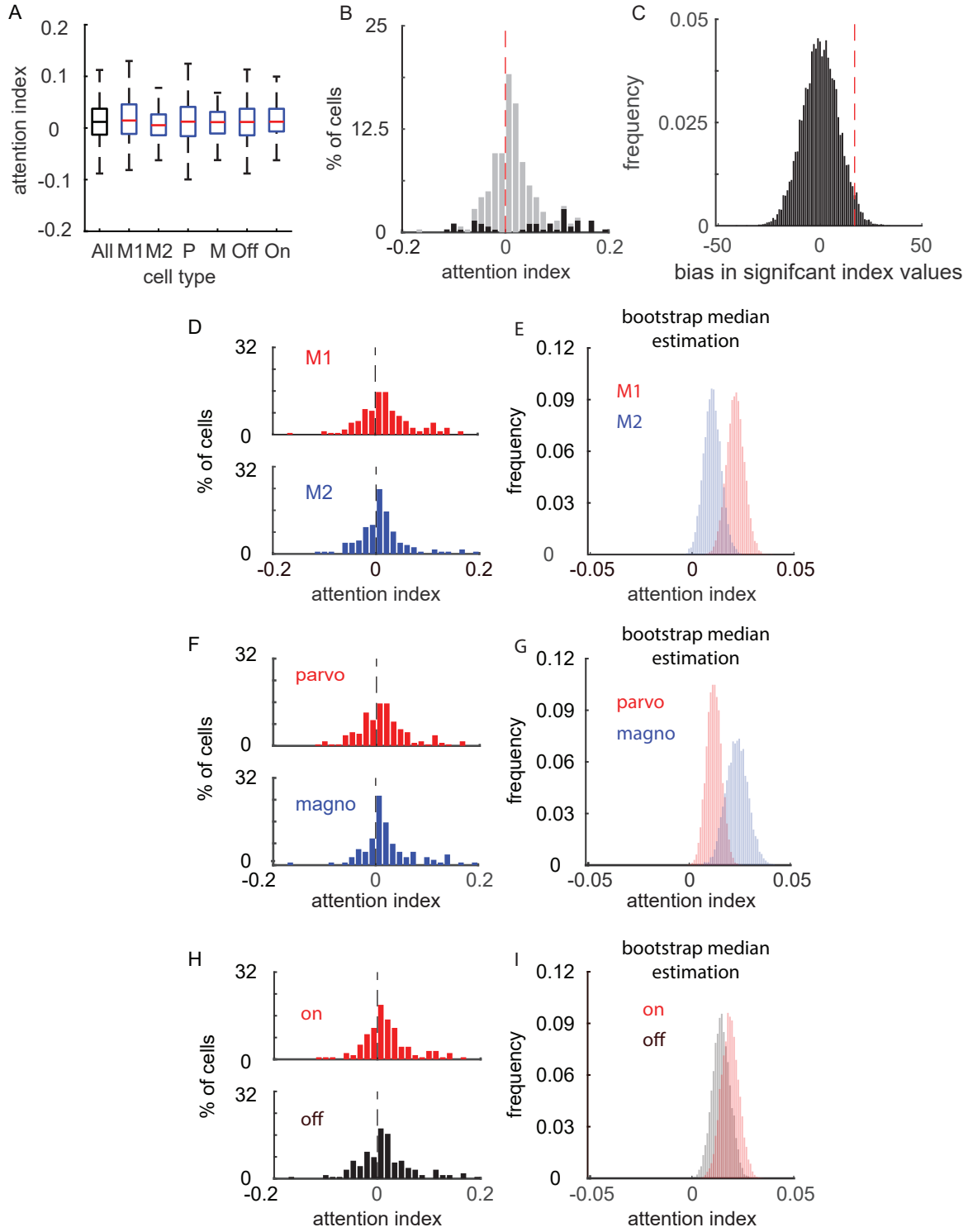
A
0.2
0.1
0
-0.1
-0.2
attention index
All M1 M2 P M Off On
cell type
B
25
12.5
0
% of cells
-0.2
0
0.2
attention index
C
0.05
0.025
0
frequency
-50
0
50
bias in signifcant index values
D
32
M1
0
32
M2
0
% of cells
-0.2
0
0.2
attention index
E
bootstrap median
estimation
0.12
0.09
0.06
0.03
0
frequency
M1
M2
-0.05
0
0.05
attention index
F
32
parvo
0
32
magno
0
% of cells
-0.2
0
0.2
attention index
G
bootstrap median
estimation
0.12
0.09
0.06
0.03
0
frequency
parvo
magno
-0.05
0
0.05
attention index
H
32
on
0
32
off
0
% of cells
-0.2
0
0.2
attention index
I
bootstrap median
estimation
0.12
0.09
0.06
0.03
0
frequency
on
off
-0.05
0
0.05
attention index

Figure 5

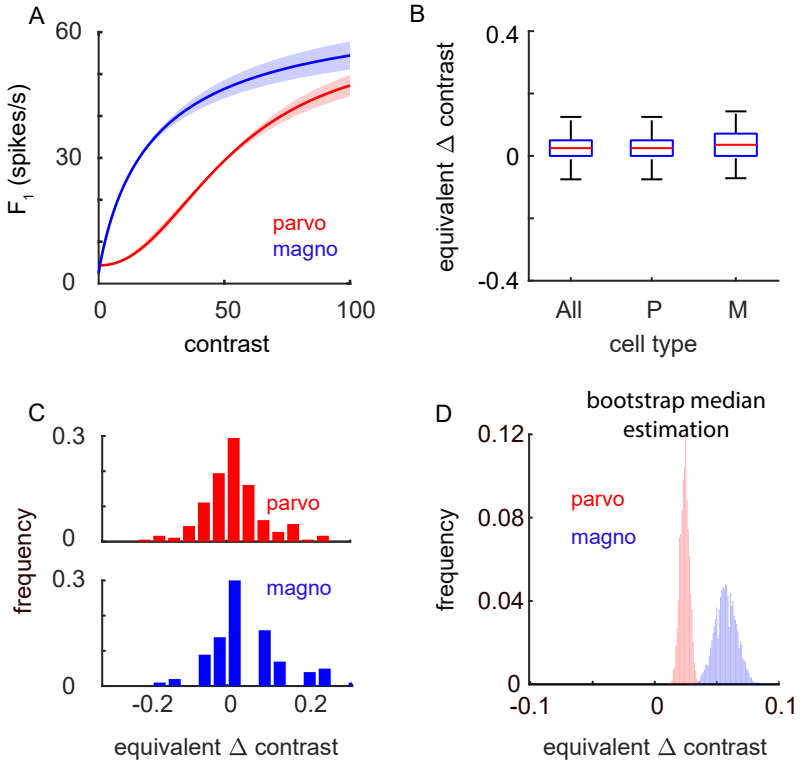
A
60
30
0
F_1 (spikes/s)
parvo
magno
0
50
100
contrast
B
0.4
0
-0.4
equivalent Δ contrast
All
P
M
cell type
C
0.3
0
frequency
parvo
0.3
0
magno
-0.2
0
0.2
equivalent Δ contrast
D
bootstrap median
estimation
0.12
0.08
0.04
0
frequency
parvo
magno
-0.1
0
0.1
equivalent Δ contrast

Figure 6

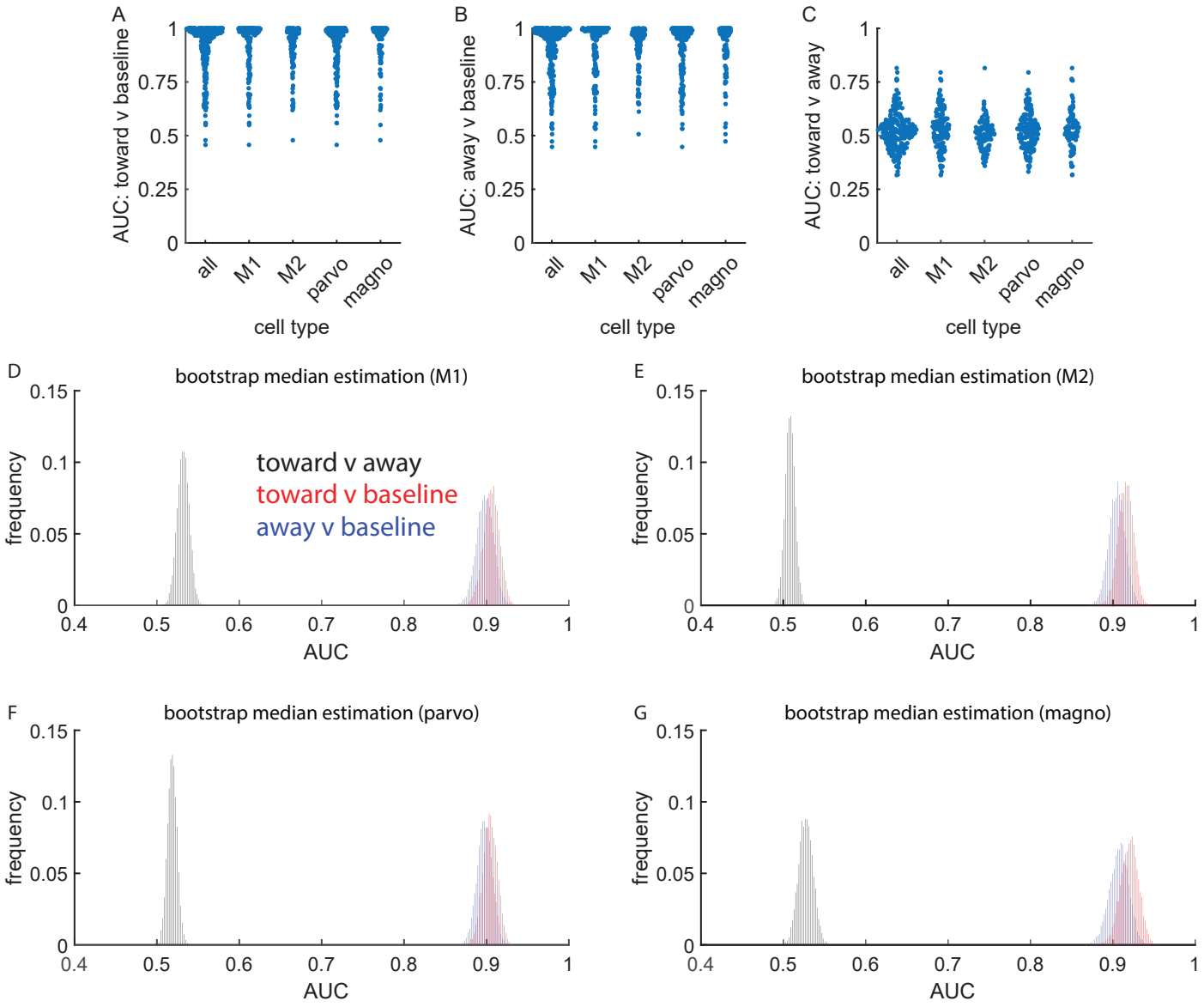
A
AUC: toward v baseline
1
0.75
0.5
0.25
0
all
M1
M2
parvo
magno
cell type
B
AUC: away v baseline
C
AUC: toward v away
D
bootstrap median estimation (M1)
frequency
0.15
0.1
0.05
toward v away
toward v baseline
away v baseline
0.4
0.5
0.6
0.7
0.8
0.9
AUC
E
bootstrap median estimation (M2)
F
bootstrap median estimation (parvo)
G
bootstrap median estimation (magno)

Figure 7

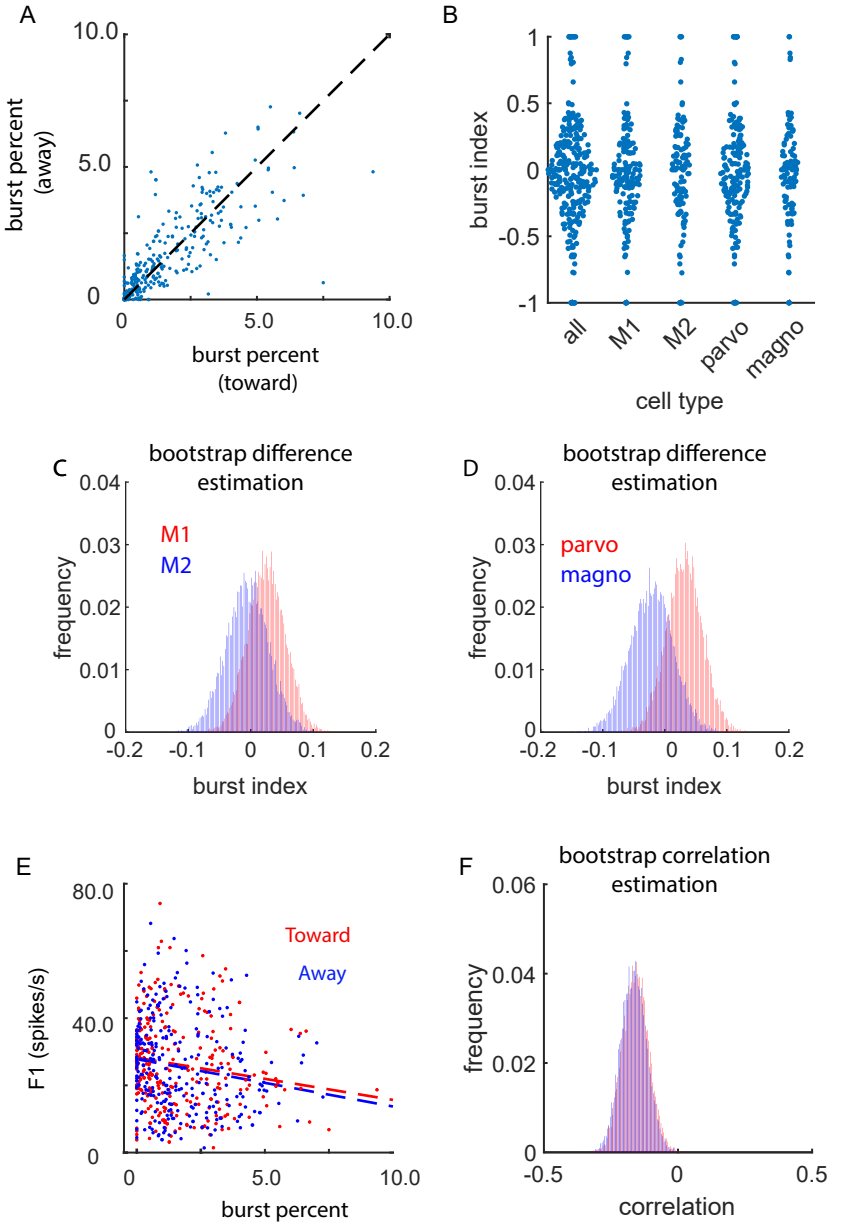
A
burst percent (away)
burst percent (toward)
B
burst index
all
M1
M2
parvo
magno
cell type
C
bootstrap difference estimation
M1
M2
frequency
burst index
D
bootstrap difference estimation
parvo
magno
frequency
burst index
E
F1 (spikes/s)
Toward
Away
burst percent
F
bootstrap correlation estimation
frequency
correlation

Figure 8

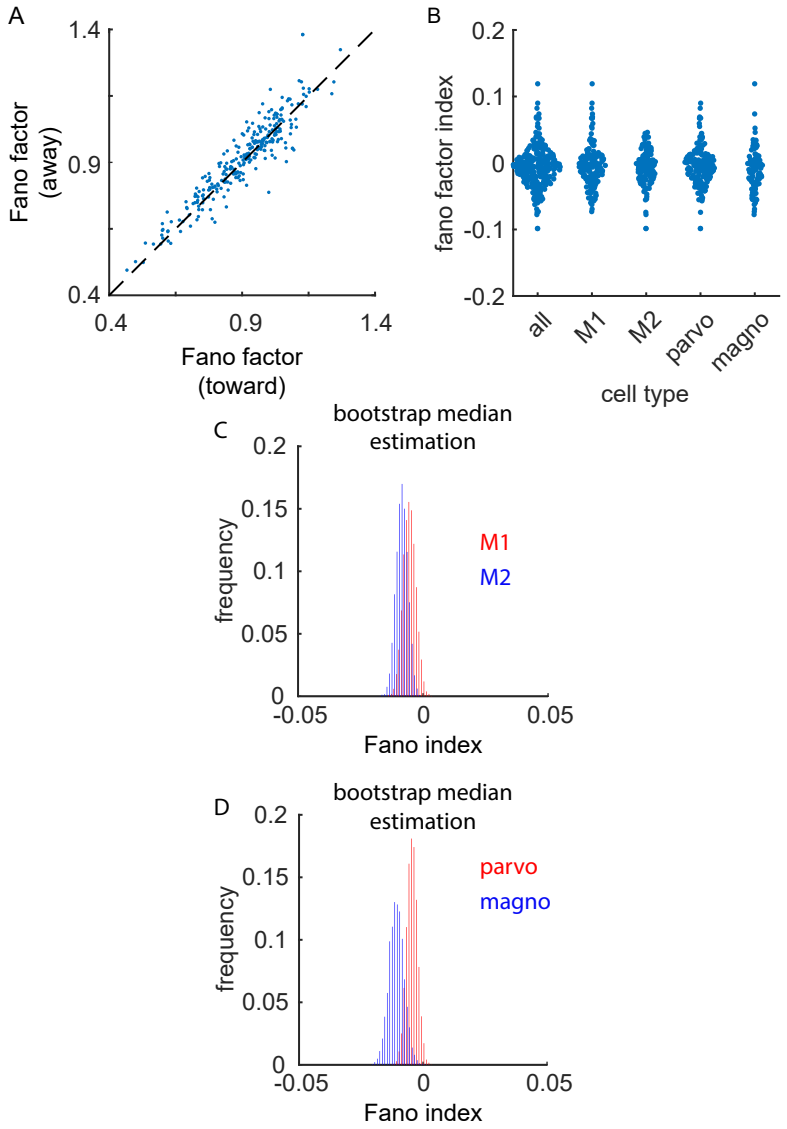
A
1.4
0.9
0.4
Fano factor (away)
0.4
0.9
1.4
Fano factor (toward)
B
0.2
0.1
0
-0.1
-0.2
fano factor index
all
M1
M2
parvo
magno
cell type
C
bootstrap median estimation
0.2
0.15
0.1
0.05
0
frequency
M1
M2
-0.05
0
0.05
Fano index
D
bootstrap median estimation
0.2
0.15
0.1
0.05
0
frequency
parvo
magno
-0.05
0
0.05
Fano index